Progress In Electromagnetics Research B, Vol. 15, 375–400, 2009

NEW VERSION OF TWA USING TWO-DIMENSIONAL NON-UNIFORM FAST FOURIER MODE TRANSFORM (2D-NUFFMT) FOR FULL-WAVE INVESTIGATION OF MICROWAVE INTEGRATED CIRCUITS

M. Ayari

Department of Mathematics
Virginia Polytechnic Institute and State University
Blacksburg, 24061-VA, USA

T. Aguili

Syscom Laboratory, Engineers' National School of Tunis
B.P 37 Le belvedere 1002, Tunis, Tunisia

H. Baudrand

EM Research & Design, RCEM
17 Rue Denis Papin 31500, Toulouse, France

Abstract—In this paper, a novel version of the transverse wave approach (TWA) based on two-dimensional non-uniform fast Fourier mode transform (2D-NUFFMT) is presented and developed for full-wave analysis of RF integrated circuits (RFICs). An adaptive mesh refinement is applied in this advanced TWA process and CPU computation time is evaluated throughout 30 GHz patch antenna, application belonging to wireless systems. The TWA in its novel version is favorably compared with the conventional one in presence of AMT technique in the context of EM simulations. Another version of TWA is outlined to illustrate a computationally efficient way to handle an arbitrary mesh for RFICs analysis with high complexity problems.

Corresponding author: M. Ayari (ayari@vt.edu).

1. INTRODUCTION

The good analysis of the numerical EM method TWA developed by our group allows us to determine not only their strong points as already mentioned in previous works [1, 2] but also their shortcomings. The weakness of TWA can be observed at an EM simulation with high precision, namely, the total number of pixels N_T exceeds 2^{18} cells ($N_T = M_x \times N_y = 512 \times 512,\ 1024 \times 1024, \ldots$); for this resolution, the FFT algorithm imposes an enormous calculation which is slows down the TWA process. Therefore, we should find efficient solution in order to tackle this problem.

Taking a glance at spatial domain in presence of considered circuit, we can notice for most applications a great loss stemming from the unexploited important number of cells, mainly outside the circuit which astoundingly increases the CPU time computation chiefly in TWA process using ultrahigh resolution. Consequently, we propose as a solution an *adaptive mesh refinement only on the domain defining the studied structure.* This can be an efficient key to resolve the emphasized problem. Yet, the discretization in the spatial domain becomes non-uniform† and the working with conventional TWA becomes impossible because the Fast Fourier Transform (FFT) which represents the spinal column of our approach solely requires an equispaced (uniform) data. Then, how could we overcome this difficulty?

In response to this question, we simply have to find a new Fourier transform dealing with non-uniform grids for computation fulfilling the two following conditions:

a. This novel Fourier transform has the possibility to process, unlike the conventional FFT, both equispaced and non-equispaced data which reduces for most applications the total number of pixels.
b. Keeping the same computational complexity as the conventional FFT algorithm that is $\mathrm{O}\left(N_T \log N_T\right)$ so as to perform the forward and inverse of this novel Fourier transform.

Based on great mathematical concepts and various scientific researches, we develop, in this paper, the novel transform named two dimensional Non-Uniform Fast Fourier Transform (2D-NUFFT) straightforwardly ensuring the transition between spatial and spectral (Fourier) domains taking into consideration the non-uniform discretization in spatial domain, and its inverse 2D-INUFFT allowing the passage from spectral domain to spatial one. The expansion of these transforms (i.e., the forward transform and its inverse) show that FMT (Fourier Mode Transform) and its inverse IFMT already

† Unlike the works presented in [1], the sizes of the cells constituting the air-dielectric interface are, in this case, unequal.

computed [1] can be associated directly to respectively 2D-NUFFT and 2D-INUFFT to form the new transformations assuring the novel pixel-mode transform and vice versa so-called two dimensional Non-Uniform Fast Fourier Mode Transform 2D-NUFFMT and its inverse 2D-INUFFMT which constitutes the fundamental base of the advanced TWA process.

A detailed description of the procedure explaining the mesh handling adopted in the iterative process of this advanced method TWA will be presented. This work will be, also, buttressed by an application belonging to wireless systems already investigated in [1] in order to show the efficiency of this advanced TWA method; moreover, the simulation time with this advanced method can be more improved by applying the AMT technique onto any considered analysis structure.

Far from the condition b. mentioned above, we conclude this work by outlining on another version of TWA method based on two dimensional Non-Uniform Discrete Fourier Transform (2D-NUDFT) using matrix form. Such a method offers the possibility to apply a special mesh on discontinuity surface that reduces considerably the CPU time computation; but unfortunately, the handling of large matrices makes TWA process slow enough which increases in turn the simulation time and causes the method to lose their reliability, trustworthiness and fastness. Therefore, *fast multiplication matrices using wavelets* can be, for example, a good solution to resolve a problem such as this and make TWA so-fast to prove its comparability with the one based on 2D-NUFFMT in terms of computation time.

2. OVERVIEW ON FOURIER TRANSFORMS

Fourier techniques[‡] have been a popular analytical tool in mathematics, mathematical physics and engineering for more than two centuries. The usefulness of such techniques is related to the trigonometric functions $e^{j\omega x}$. These are eigenfunctions of the differentiation operator and can be efficiently utilized to model solutions of differential equations which arise in the fields mentioned above.

The discovery, popularization, and digital realization of fast algorithms for Fourier analysis — so called FFT — have had far reaching implications in science and technology in recent decades. The scientific computing community has established Fourier analysis as a

‡ Fourier techniques or Fourier transforms provide a way to convert samples of a standard time-series into the frequency domain. This provides a dual representation of the function, in which certain operations become easier than in the time domain. Their applications include filtering, image compression, convolution/deconvolution and computing the correlation of functions; more details can be found in [6].

powerful and practical numerical tool and regards the FFT as one of the leading algorithmic achievements of the 20th century [3, 4].

In fact, Fast Fourier transform (FFT) has been enjoying widespread applications in antennas, scattering, and computational electromagnetics, as well as in signal and image processing and other areas of computational science and engineering since Cooley and Tukey [5] established, in the 1960s, a powerful algorithm for fast calculation of Fourier transforms. Its algorithm provides an accurate way to evaluate the discrete Fourier transform (DFT) of a sequence of N uniformly spaced samples in $\mathrm{O}(N \log N)$ time.

However, the urgent requirement of input data with not uniformly (i.e., not equally) spaced, a condition that is required for the FFT, in many practical situations implies the appearance of non-equispaced (non-uniform) fast Fourier transform which is a generalization of the fast Fourier transformation (FFT) for data located on non-equispaced grids[§]. Indeed, the idea of non-uniform frequency sampling has helped Scientifics' engineers and researchers to solve problems encountered in various applications chiefly in spectral processing [8, 9] and filter design [10–12].

Hence, the NUFFT has recently been presented in several applications in medical imaging. For instance, it is used in magnetic resonance imaging (MRI) for reconstruction of data located on spiral or radial trajectories [13, 14]; moreover, it can be found in such applications such as astronomy [15], tomography [16–18], ultrasound [19] and so forth.

The Fourier transform with non-uniformly sampled data can be computed directly by its conventional definition, but their well-known properties such as the orthogonality of exponential basis, symmetry and so on are not generally valid and the FFT algorithm cannot be applied in this case. To overcome this limitation, Dutt and Rokhlin [20, 21], Beylkin [22] and Steidl [23, 24] studied the problem of forward FFT for unequally spaced data. The results obtained in [23, 24] provide high accuracies and fast calculation for nonuniform FFT (NUFFT) in unidimensional problem.

In what follows, based on Dutt-Rokhlin interpolation method[‖] [20] and the theoretical background of diverse mathematical concepts, we will develop the two-dimensional non-equispased fast Fourier transform (2D-NUFFT) as well as its inverse in order to implement them

[§] Overall, neither the speed nor the accuracy of the FFT can be duplicated in the case of non-uniformly sampled data. Algorithms to evaluate the DFT for non-uniform data typically employ an approximation scheme, with increased accuracy available at the cost of increased execution time [7].

[‖] Some errors are found in this method and corrected with the help of professors S. Adjerid and D. Russell in the department of mathematics at Virginia tech.

straightforwardly in our numerical EM method TWA¶.

It should be noted that finding the inverse of NUFFT is a very difficult task. Therefore, up-to-now their existence is hardly absent in literature (except the one investigated in [25, 42] in one dimensional case or the one using the matrix form which will be presented later) in view of their limitation or needlessness in most areas of computational science and engineering.

We will also show that the computational complexity algorithms of 2D-NUFFT as well as its inverse are equal to the one of the conventional two-dimensional fast Fourier transform (2D-FFT).

3. TWO-DIMENSIONAL NON-UNIFORM FAST FOURIER TRANSFORM (2D-NUFFT)

Given $C = \{C_{mn}\}_{\substack{0\leq m\leq M-1\\0\leq n\leq N-1}}$ sequence of $M \times N$ complex numbers, the two-dimensional Fourier transform as a general rule of discretely sampled data of the transformation $F : \mathbb{C}^{M\times N} \to \mathbb{C}^{M\times N}$ is defined by the following formulae:

$$F\left(C\right)_{k,l} = h\left(x_k, y_l\right) = \sum_{\substack{0\leq m\leq M-1\\0\leq n\leq N-1}} C_{mn} \cdot e^{j(m\cdot x_k+n\cdot y_l)} \tag{1}$$

for $k = 0, \ldots, M-1$ and $l = 0, \ldots, N-1$, where $x = \{x_0, \ldots, x_{M-1}\}$ and $y = \{y_0, \ldots, y_{N-1}\}$ are both sequences of real numbers in $[0, 2\pi]$.

We will consider throughout this section the two distinct sets of points as follows:

In the first set: let $\left\{\overset{u}{x}_0, \ldots, \overset{u}{x}_{M-1}\right\}$ and $\left\{\overset{u}{y}_0, \ldots, \overset{u}{y}_{N-1}\right\}$ be sequences of *equispaced* real numbers in the interval $[0, 2\pi]$ as:

$$\begin{cases} \overset{u}{x}_k = \frac{2\pi k}{M}; 0 \leq k \leq M-1 \\ \overset{u}{y}_l = \frac{2\pi l}{N}; 0 \leq l \leq N-1 \end{cases} \tag{2}$$

where u designates the uniformity of input data (i.e., the data are equally spaced).

In the second set: let $\left\{\overset{nu}{x}_0, \ldots, \overset{nu}{x}_{M-1}\right\}$ and $\left\{\overset{nu}{y}_0, \ldots, \overset{nu}{y}_{N-1}\right\}$ be sequences of *non-uniformly spaced* real numbers in the interval $[0, 2\pi]$

¶ We do not know hitherto any numerical EM method developed in literature which has used NUFFT except the work presented by K. Y. Su and J. T. Kuo (see [26, 27]) who incorporated the forward 2D-NUFFT into both method of moment (MoM) and spectral domain approach (SDA) for analysis of microwave circuits and the work of Q. H. Liu et al. [28] who applied the forward NUFFT and related fast transform algorithms to numerical solutions of Maxwell's equations in time and frequency domains.

where nu indicates the non-uniformity of input data (i.e., unequally spaced data).

Using (2) in (1), we obtain the two-dimensional inverse discrete Fourier transform (2D-IDFT):

$$\underbrace{f_{k,l}}_{Spatial\ domain} = h\left(\overset{u}{x}_k, \overset{u}{y}_l\right) = \sum_{\substack{0\le m\le M-1\\0\le n\le N-1}} \underbrace{C_{mn}}_{Frquencydomain} \cdot e^{j\left(m\cdot\overset{u}{x}_k + n\cdot\overset{u}{y}_l\right)} \tag{3}$$

for $k = 0, \ldots, M-1$ and $l = 0, \ldots, N-1$.

From (3), the forward 2D-DFT can be written as:

$$C_{mn} = \frac{1}{M\times N}\sum_{\substack{0\le k\le M-1\\0\le l\le N-1}} f_{k,l}\cdot e^{-j\left(m\cdot\overset{u}{x}_k + n\cdot\overset{u}{y}_l\right)} \tag{4}$$

Let $N_T = M\times N$ be a total number of input data.

It is understandable that the 2D-FFT algorithm should be employed in order to reduce the number of operations for 2D-DFT from $\mathrm{O}\left(N_T^2\right)$ to $\mathrm{O}\left(N_T \log N_T\right)$.

Furthermore, using the notation mentioned above for the non-uniform case, (1) yields

$$\underbrace{g_{p,q}}_{Spatial\ domain} = h\left(\overset{nu}{x}_p, \overset{nu}{y}_q\right) = \sum_{\substack{0\le m\le M-1\\0\le n\le N-1}} \underbrace{C_{mn}}_{Frquency\ domain} \cdot e^{j\left(m\cdot\overset{nu}{x}_p + n\cdot\overset{nu}{y}_q\right)} \tag{5}$$

for $p = 0, \ldots, M-1$ and $q = 0, \ldots, N-1$.

The exponential base $\left\{e^{j\left(m\cdot\overset{nu}{x}_k + n\cdot\overset{nu}{y}_l\right)}\right\}_{m,n}$ constitutes a non-orthogonal basis+. Therefore, the inverse of (5) cannot be obtained by simple '-' sign introduced in exponential like conventional DFT.

We will seek a fast method ensuring the transition between spatial and frequency domains in the case of non-uniformly sampled data; in other words, a mathematical transformation which allows the quick finding of the coefficients $\{C_{mn}\}_{\substack{0\le m\le M-1\\0\le n\le N-1}}$ from $\{g_{pq}\}_{\substack{0\le m\le M-1\\0\le n\le N-1}}$ and vice versa.

+ $\left\langle e^{j\left(m\cdot\overset{nu}{x}_k + n\cdot\overset{nu}{y}_l\right)} \,\middle|\, e^{j\left(r\cdot\overset{nu}{x}_k + s\cdot\overset{nu}{y}_l\right)}\right\rangle \neq 0$ for $(m,n)\neq(r,s)$

Then, inserting (4) in (5) we obtain

$$g_{p,q} = \sum_{\substack{0\le m\le M-1\\0\le n\le N-1}} \frac{1}{M\times N} \sum_{\substack{0\le m\le M-1\\0\le n\le N-1}} f_{k,l}\cdot e^{-j\left(m\cdot \overset{u}{x}_k + n\cdot \overset{u}{y}_l\right)} e^{j\left(m\cdot \overset{nu}{x}_p + n\cdot \overset{nu}{y}_q\right)} \tag{6}$$

for $p = 0, \ldots, M-1$ and $q = 0, \ldots, N-1$.

This can be rewritten in reduced form as:

$$g_{p,q} = \sum_{\substack{0\le m\le M-1\\0\le n\le N-1}} \mathrm{K}_{k,l}^{p,q}\cdot f_{k,l} \tag{7}$$

for $p = 0, \ldots, M-1$ and $q = 0, \ldots, N-1$, where the expression of $\mathrm{K}_{k,l}^{p,q}$ for $k, p = 0, \ldots, M-1$ and $q, l = 0, \ldots, N-1$ is given by:

$$\mathrm{K}_{k,l}^{p,q} = \frac{1}{M\times N} \sum_{\substack{0\le m\le M-1\\0\le n\le N-1}} e^{jm\left(\overset{nu}{x}_p - \overset{u}{x}_k\right)} \cdot e^{jn\left(\overset{nu}{y}_q - \overset{u}{y}_l\right)} \tag{8}$$

Using the properties of sum, (8) can be expressed as:

$$\mathrm{K}_{k,l}^{p,q} = \frac{1}{M\times N}\left[\sum_{m=0}^{M-1}\left(e^{j\left(\overset{nu}{x}_p - \overset{u}{x}_k\right)}\right)^m\right]\cdot\left[\sum_{n=0}^{N-1}\left(e^{j\left(\overset{nu}{y}_q - \overset{u}{y}_l\right)}\right)^n\right] \tag{9}$$

Computing (9) while taking into consideration all possible cases stemmed from the working out of two geometric series well-observed in the expression of this equation and the properties of the exponential, we obtain the following result:

$$K_{k,l}^{pq} = \begin{cases} F_{p,q}\cdot G(\overset{nu}{x}_p - \overset{u}{x}_k)G(\overset{nu}{y}_q - \overset{u}{y}_l);\ \overset{nu}{x}_p \neq \overset{u}{x}_k \ and\ \overset{nu}{y}_q \neq \overset{u}{y}_l \\ \tilde{F}_p\cdot G(\overset{nu}{x}_p - \overset{u}{x}_k);\ \overset{nu}{x}_p \neq \overset{u}{x}_k \ and\ \overset{nu}{y}_q = \overset{u}{y}_l \\ F_q\cdot G(\overset{nu}{y}_q - \overset{u}{y}_l);\ \overset{nu}{x}_p = \overset{u}{x}_k \ and\ \overset{nu}{y}_q \neq \overset{u}{y}_l \\ 1;\ \overset{nu}{x}_p = \overset{u}{x}_k \ and\ \overset{nu}{y}_q = \overset{u}{y}_l \end{cases} \tag{10}$$

for $k, p = 0, \ldots, M-1$ and $q, l = 0, \ldots, N-1$.

Where

$$\tilde{F}_p = \left(\frac{e^{iM\overset{nu}{x}_p} - 1}{M}\right) \tag{11}$$

$$F_q = \left(\frac{e^{iN\overset{nu}{y_q}} - 1}{N}\right) \tag{12}$$

$$F_{p,q} = \tilde{F}_p \cdot F_q \tag{13}$$

$$G(t) = \frac{1}{e^{it} - 1};\ t \neq 0 \tag{14}$$

Returning to (7), we notice that this equation offers the possibility to effectively transform the coefficients defined with equispaced data $\{f_{k,l}\}$ into the one with unequally data $\{g_{p,q}\}$; $\{f_{k,l}\}$ coefficients can be computed obviously from $\{C_{m,n}\}$ coefficients according to (3).

The scheme depicted in Figure 1 summarizes the steps mentioned above.

$$\underbrace{\left\{C_{m,n}\right\}_{\substack{0\le m\le M-1\\ 0\le n\le N-1}}}_{\text{Spectral Domain}} \xrightarrow{(6.3)} \left\{f_{k,l}\right\}_{\substack{0\le k\le M-1\\ 0\le l\le N-1}} \xrightarrow{(6.7)} \underbrace{\left\{g_{p,q}\right\}_{\substack{0\le p\le M-1\\ 0\le q\le N-1}}}_{\text{Spatial Domain}}$$

Figure 1. Transformation from spectral domain to spatial domain for non-uniformly sampled data.

It should be noted that the speed of computation algorithm of this transformation will be mentioned later. To ensure the transition between spatial and spectral domain, we should fulfill the scheme shown below:

$$\underbrace{\left\{g_{p,q}\right\}_{\substack{0\le p\le M-1\\ 0\le q\le N-1}}}_{\text{Spatial Domain}} \xrightarrow{?} \left\{f_{k,l}\right\}_{\substack{0\le k\le M-1\\ 0\le l\le N-1}} \xrightarrow{(6.4)} \underbrace{\left\{C_{m,n}\right\}_{\substack{0\le m\le M-1\\ 0\le n\le N-1}}}_{\text{Spectral Domain}}$$

Figure 2. Transition from spatial domain to spectral domain for non-uniformly sampled data.

Rewriting (7) on the following form:

$$\{g_{p,q}\} = \left\{\mathrm{K}_{k,l}^{p,q}\right\}\{f_{k,l}\} \tag{15}$$

and $\{f_{k,l}\}$ coefficients can be expressed from (15) as follows:

$$\{f_{k,l}\} = \left\{\mathrm{K}_{k,l}^{p,q}\right\}^{-1}\{g_{p,q}\} = \left\{L_{p,q}^{k,l}\right\}\{g_{p,q}\} \tag{16}$$

Find, hence, $\left\{L_{p,q}^{k,l}\right\}$?

Indeed, let $\{\alpha_{ij}\}_{\substack{0\leq m\leq M-1\\0\leq n\leq N-1}}$ be a sequence of complex number.

Further, let $\left\{\overset{x}{\omega}_0,\ldots,\overset{x}{\omega}_{M-1}\right\}$, $\left\{\overset{y}{\omega}_0,\ldots,\overset{y}{\omega}_{N-1}\right\}$, $\left\{\overset{x}{Z}_0,\ldots,\overset{x}{Z}_{M-1}\right\}$ and $\left\{\overset{y}{Z}_0,\ldots,\overset{y}{Z}_{N-1}\right\}$ be sequences of complex numbers defined by the formulae:

$$\overset{x}{\omega}_k = e^{j\,\overset{u}{x}_k};\quad \overset{y}{\omega}_l = e^{j\,\overset{u}{y}_l} \tag{17}$$

$$\overset{x}{Z}_p = e^{j\,\overset{nu}{x}_p};\quad \overset{y}{Z}_q = e^{j\,\overset{nu}{y}_q} \tag{18}$$

for $k,p = 0,\ldots,M-1$ and $q,l = 0,\ldots,N-1$.

We suppose, according to (1) with translation, that

$$\begin{cases} f_{k,l} = \displaystyle\sum_{\substack{-\frac{M}{2}\leq m\leq\frac{M}{2}-1\\-\frac{N}{2}\leq n\leq\frac{N}{2}-1}} \alpha_{mn}\cdot e^{j\left(m\cdot\overset{u}{x}_k+n\cdot\overset{u}{y}_l\right)} \\ g_{p,q} = \displaystyle\sum_{\substack{-\frac{M}{2}\leq m\leq\frac{M}{2}-1\\-\frac{N}{2}\leq n\leq\frac{N}{2}-1}} \alpha_{mn}\cdot e^{j\left(m\cdot\overset{nu}{x}_p+n\cdot\overset{nu}{y}_q\right)} \end{cases} \tag{19}$$

for $k,p = 0,\ldots,M-1$ and $q,l = 0,\ldots,N-1$.

Let the polynomial $\mathbf{P}_\alpha$ be defined by the following formula:

$$\mathbf{P}_\alpha(u,v) = \sum_{\substack{0\leq m\leq M-1\\0\leq n\leq N-1}} \alpha_{m-\frac{M}{2},n-\frac{N}{2}}\cdot u^m\cdot v^n \tag{20}$$

The values of the polynomial $\mathbf{P}_\alpha$ at the points $\left\{\overset{x}{\omega}_k,\overset{y}{\omega}_l\right\}$ to the values at the points $\left\{\overset{x}{Z}_p,\overset{y}{Z}_q\right\}$ can be obtained by the *interpolation method.* In literature, we have numerous methods that handle this kind of interpolation belonging to the set of two dimensional interpolation methods (see [29]). For the current problem, we selected the *2D-Lagrange Interpolation Formula* (2D-LIF) which is an extension of 1D-LIF by applying on it a *tensor product technique* [30].

Therefore, the 2D-LIF relating the values of $\mathbf{P}_\alpha$ at the points $\left\{\overset{x}{\omega}_k,\overset{y}{\omega}_l\right\}$ to the values at the points $\left\{\overset{x}{Z}_p,\overset{y}{Z}_q\right\}$ can be expressed as follows:

$$\mathbf{P}_\alpha\left(\overset{x}{\omega}_k, \overset{y}{\omega}_l\right) = \sum_{\substack{p=1,\dots,M\\q=1,\dots,N}} \mathbf{P}_\alpha\left(\overset{x}{Z}_p, \overset{y}{Z}_q\right) L_{p,q}\left(\overset{x}{\omega}_k, \overset{y}{\omega}_l\right)$$
$$= \sum_{\substack{p=1,\dots,M\\q=1,\dots,N}} \mathbf{P}_\alpha\left(\overset{x}{Z}_p, \overset{y}{Z}_q\right) L_p\left(\overset{x}{\omega}_k\right) \tilde{L}_q\left(\overset{y}{\omega}_l\right) \tag{21}$$

for $k = 0, \dots, M-1$ and $l = 0, \dots, N-1$.

Where

$$L_p(x) = \prod_{\substack{k=1\\k\neq p}}^{M} \left(\frac{x - \overset{x}{Z}_k}{\overset{x}{Z}_p - \overset{x}{Z}_k}\right); \quad p \in [\![1, \dots, M]\!] \tag{22}$$

$$\tilde{L}_q(x) = \prod_{\substack{k=1\\k\neq q}}^{N} \left(\frac{x - \overset{y}{Z}_k}{\overset{y}{Z}_q - \overset{y}{Z}_k}\right); \quad q \in [\![1, \dots, N]\!] \tag{23}$$

$$L_{p,q}(x, y) = L_p(x) \cdot \tilde{L}_q(y) \tag{24}$$

for $p = 1, \dots, M$ and $q = 1, \dots, N$.

The numerator of (22) at points $\left\{\overset{x}{\omega}_k\right\}$; $k \in [\![1, \dots, M]\!]$ is given by:

$$\prod_{\substack{i=1\\i\neq p}}^{M} \left(\overset{x}{\omega}_k - \overset{x}{Z}_i\right) = \prod_{\substack{i=1\\i\neq p}}^{M} \left(e^{j\,\overset{u}{x}_k} - e^{j\,\overset{nu}{x}_i}\right) \tag{25}$$

With the fact that $\left\{\begin{array}{l} X = \left(\frac{X+Y}{2}\right) + \left(\frac{X-Y}{2}\right) \\ Y = \left(\frac{X+Y}{2}\right) - \left(\frac{X-Y}{2}\right) \end{array}\right\}$, (25) becomes

$$\prod_{\substack{i=1\\i\neq p}}^{M} \left(\overset{x}{\omega}_k - \overset{x}{Z}_i\right) = \prod_{\substack{i=1\\i\neq p}}^{M} e^{j\left(\overset{u}{x}_k + \overset{nu}{x}_i\right)/2} \left(e^{j\left(\overset{u}{x}_k - \overset{nu}{x}_i\right)/2} - e^{-j\left(\overset{u}{x}_k - \overset{nu}{x}_i\right)/2}\right) \tag{26}$$

Using the trigonometric properties, (26) yields:

$$\prod_{\substack{i=1\\i\neq p}}^{M} \left(\overset{x}{\omega}_k - \overset{x}{Z}_i\right) = 2j \times e^{j\frac{(M-1)\,\overset{u}{x}_k}{2}} \prod_{\substack{i=1\\i\neq p}}^{M} \left(e^{j\frac{\overset{nu}{x}_i}{2}} \cdot \sin\left(\left(\overset{u}{x}_k - \overset{nu}{x}_i\right)/2\right)\right) \tag{27}$$

From (17) and (18), we get

$$\prod_{\substack{i=1\\ i\neq p}}^{M}\left(\overset{x}{\omega}_k-\overset{x}{Z}_i\right)=2j\times\overset{x}{\omega}_k{}^{\left(\frac{M-1}{2}\right)}\prod_{\substack{i=1\\ i\neq p}}^{M}\left(\overset{x}{Z}_i{}^{1/2}\cdot\sin\left(\left(\overset{u}{x}_k-\overset{nu}{x}_i\right)\Big/2\right)\right)\tag{28}$$

Replacing $\overset{x}{Z}_p$ and $\overset{nu}{x}_p$ respectively by $\overset{x}{\omega}_k$ and $\overset{u}{x}_k$ in (27), we, hence, obtain

$$\prod_{\substack{i=1\\ i\neq p}}^{M}\left(\overset{x}{Z}_p-\overset{x}{Z}_i\right)=2j\times e^{j\frac{(M-1)\overset{nu}{x}_p}{2}}\prod_{\substack{i=1\\ i\neq p}}^{M}\left(e^{j\frac{\overset{nu}{x}_i}{2}}\cdot\sin\left(\left(\overset{nu}{x}_p-\overset{nu}{x}_i\right)\Big/2\right)\right)\tag{29}$$

And also from (18), we get

$$\prod_{\substack{i=1\\ i\neq p}}^{M}\left(\overset{x}{Z}_p-\overset{x}{Z}_i\right)=2j\times\overset{x}{Z}_p{}^{\left(\frac{M-1}{2}\right)}\prod_{\substack{i=1\\ i\neq p}}^{M}\left(\overset{x}{Z}_i{}^{1/2}\cdot\sin\left(\left(\overset{nu}{x}_p-\overset{nu}{x}_i\right)\Big/2\right)\right)\tag{30}$$

In the same way, we have

$$\prod_{\substack{i=1\\ i\neq p}}^{M}\left(\overset{y}{\omega}_l-\overset{y}{Z}_i\right)=2j\times\overset{y}{\omega}_l{}^{\left(\frac{M-1}{2}\right)}\prod_{\substack{i=1\\ i\neq p}}^{M}\left(\overset{y}{Z}_i{}^{1/2}\cdot\sin\left(\left(\overset{u}{y}_l-\overset{nu}{y}_i\right)\Big/2\right)\right)\tag{31}$$

$$\prod_{\substack{i=1\\ i\neq q}}^{M}\left(\overset{y}{Z}_q-\overset{y}{Z}_i\right)=2j\times\overset{y}{Z}_q{}^{\left(\frac{M-1}{2}\right)}\prod_{\substack{i=1\\ i\neq q}}^{M}\left(\overset{y}{Z}_i{}^{1/2}\cdot\sin\left(\left(\overset{nu}{y}_q-\overset{nu}{y}_i\right)\Big/2\right)\right)\tag{32}$$

From (28) and (30), (22) at points $\left\{\overset{x}{\omega}_k\right\}$; $k\in[\![1,\ldots,M]\!]$ becomes:

$$L_p\left(\overset{x}{\omega}_k\right)=\frac{\prod\limits_{\substack{i=1\\ i\neq p}}^{M}\left(\overset{x}{\omega}_k-\overset{x}{Z}_i\right)}{\prod\limits_{\substack{i=1\\ i\neq p}}^{M}\left(\overset{x}{Z}_p-\overset{x}{Z}_i\right)}=\underbrace{\frac{\overset{x}{\omega}_k{}^{\left(\frac{M-1}{2}\right)}}{\overset{x}{Z}_p{}^{\left(\frac{M-1}{2}\right)}}}_{\text{1st } term}\times\prod_{\substack{i=1\\ i\neq p}}^{M}\frac{\sin\left(\left(\overset{u}{x}_k-\overset{nu}{x}_i\right)\Big/2\right)}{\sin\left(\left(\overset{nu}{x}_p-\overset{nu}{x}_i\right)\Big/2\right)}\tag{33}$$

The calculation of the 1st term of (33) is given as follows:

$$\frac{\overset{x}{\omega}_k{}^{\left(\frac{M-1}{2}\right)}}{\overset{x}{Z}_p{}^{\left(\frac{M-1}{2}\right)}}=\left(\frac{\overset{x}{\omega}_k}{\overset{x}{Z}_p}\right)^{M/2}\cdot\overset{x}{\omega}_k{}^{-1/2}\cdot\overset{x}{Z}_p{}^{1/2}\tag{34}$$

Using (17) and (18), we get:

$$\frac{\overset{x}{\omega}_k^{\left(\frac{M-1}{2}\right)}}{\overset{x}{Z}_p^{\left(\frac{M-1}{2}\right)}} = \left(\frac{\overset{x}{\omega}_k}{\overset{x}{Z}_p}\right)^{M/2} \cdot e^{-j\left(\overset{u}{x}_k - \overset{nu}{x}_p\right)/2} \tag{35}$$

Inserting (35) in (33), we obtain

$$L_p\left(\overset{x}{\omega}_k\right) = \left(\frac{\overset{x}{\omega}_k}{\overset{x}{Z}_p}\right)^{M/2} \cdot e^{-j\left(\overset{u}{x}_k - \overset{nu}{x}_p\right)/2} \times \prod_{\substack{i=1\\ i\neq p}}^{M} \frac{\sin\left(\left(\overset{u}{x}_k - \overset{nu}{x}_i\right)/2\right)}{\sin\left(\left(\overset{nu}{x}_p - \overset{nu}{x}_i\right)/2\right)}; \quad k, p \in [\![1, \ldots, M]\!] \tag{36}$$

For $\overset{u}{x}_k \neq \overset{nu}{x}_p \forall k, p \in [\![1, \ldots, M]\!]$, (36) can be rewritten as:

$$L_p\left(\overset{x}{\omega}_k\right) = \left(\frac{\overset{x}{\omega}_k}{\overset{x}{Z}_p}\right)^{M/2} \cdot \frac{e^{-j\left(\overset{u}{x}_k - \overset{nu}{x}_p\right)/2}}{\sin\left(\left(\overset{u}{x}_k - \overset{nu}{x}_p\right)/2\right)} \cdot \frac{\prod_{i=1}^{M} \sin\left(\left(\overset{u}{x}_k - \overset{nu}{x}_i\right)/2\right)}{\prod_{\substack{i=1\\ i\neq p}}^{M} \sin\left(\left(\overset{nu}{x}_p - \overset{nu}{x}_i\right)/2\right)}; \quad k, p \in [\![1, \ldots, M]\!] \tag{37}$$

Or,

$$\begin{aligned} \frac{e^{-j\left(\overset{u}{x}_k - \overset{nu}{x}_p\right)/2}}{\sin\left(\left(\overset{u}{x}_k - \overset{nu}{x}_p\right)/2\right)} &= \frac{\cos\left(\left(\overset{u}{x}_k - \overset{nu}{x}_p\right)/2\right) - j\sin\left(\left(\overset{u}{x}_k - \overset{nu}{x}_p\right)/2\right)}{\sin\left(\left(\overset{u}{x}_k - \overset{nu}{x}_p\right)/2\right)} \\ &= \cot\left(\frac{\overset{u}{x}_k - \overset{nu}{x}_p}{2}\right) - j \end{aligned} \tag{38}$$

Therefore for $\overset{u}{x}_k \neq \overset{nu}{x}_p$; $k, p \in [\![1, \ldots, M]\!]$ and $\overset{u}{y}_l \neq \overset{nu}{y}_q$; $l, q \in [\![1, \ldots, N]\!]$, the general expressions of $L_p(x)$ and $\tilde{L}_q(x)$ at, respectively, the points $\left\{\overset{x}{\omega}_k\right\}$; $k \in [\![1, \ldots, M]\!]$ and the points $\left\{\overset{y}{\omega}_l\right\}$; $l \in [\![1, \ldots, N]\!]$ are given as follows:

$$L_p\left(\overset{x}{\omega}_k\right) = \left(\frac{\overset{x}{\omega}_k}{\overset{x}{Z}_p}\right)^{M/2} \cdot \left[\cot\left(\frac{\overset{u}{x}_k - \overset{nu}{x}_p}{2}\right) - j\right] \cdot \frac{\prod_{i=1}^{M} \sin\left(\left(\overset{u}{x}_k - \overset{nu}{x}_i\right)/2\right)}{\prod_{\substack{i=1\\ i\neq p}}^{M} \sin\left(\left(\overset{nu}{x}_p - \overset{nu}{x}_i\right)/2\right)}; \quad k, p \in [\![1, \ldots, M]\!] \tag{39}$$

and

$$\tilde{L}_q\left(\overset{y}{\omega}_l\right)=\left(\frac{\overset{y}{\omega}_l}{\overset{y}{Z}_q}\right)^{N/2}\cdot\left[\cot\left(\frac{\overset{u}{y}_l-\overset{nu}{y}_q}{2}\right)-j\right]\cdot\frac{\prod\limits_{i=1}^{N}\sin\left(\left(\overset{u}{y}_l-\overset{nu}{y}_i\right)\Big/2\right)}{\prod\limits_{\substack{i=1\\ i\neq q}}^{N}\sin\left(\left(\overset{nu}{y}_q-\overset{nu}{y}_i\right)\Big/2\right)};$$

$$l,q\in[\![1,\ldots,N]\!] \tag{40}$$

And the expression of $L_{p,q}(x,y)$, at the points $\left\{\overset{x}{\omega}_k,\overset{y}{\omega}_l\right\}$ in the case of $\overset{u}{x}_k\neq\overset{nu}{x}_p$ and $\overset{u}{y}_l\neq\overset{nu}{y}_q$ for $k,p=1,\ldots,M$ and $l,q=1,\ldots,N$, becomes:

$$\begin{aligned}L_{p,q}\left(\overset{x}{\omega}_k,\overset{y}{\omega}_l\right)=&\ \overset{x}{\omega}_k{}^{M/2}\cdot\overset{y}{\omega}_l{}^{N/2}\cdot\overset{x}{Z}_p{}^{-M/2}\cdot\overset{y}{Z}_q{}^{-N/2}\cdot c_{k,l}\cdot d_{p,q}\\ &\cdot\left[\cot\left(\frac{\overset{u}{x}_k-\overset{nu}{x}_p}{2}\right)-j\right]\cdot\left[\cot\left(\frac{\overset{u}{y}_l-\overset{nu}{y}_q}{2}\right)-j\right]\end{aligned} \tag{41}$$

where

$$c_{k,l}=c_k\times c_l=\underbrace{\left[\prod_{i=1}^{M}\sin\left(\left(\overset{u}{x}_k-\overset{nu}{x}_i\right)\Big/2\right)\right]}_{c_k}\times\underbrace{\left[\prod_{i=1}^{N}\sin\left(\left(\overset{u}{y}_l-\overset{nu}{y}_i\right)\Big/2\right)\right]}_{c_l} \tag{42}$$

and

$$d_{p,q}=d_p\times d_q=\underbrace{\left[\prod_{\substack{i=1\\ i\neq p}}^{M}\frac{1}{\sin\left(\left(\overset{nu}{x}_p-\overset{nu}{x}_i\right)\Big/2\right)}\right]}_{d_p}\times\underbrace{\left[\prod_{\substack{i=1\\ i\neq q}}^{N}\frac{1}{\sin\left(\left(\overset{nu}{y}_q-\overset{nu}{y}_i\right)\Big/2\right)}\right]}_{d_q} \tag{43}$$

Returning to (21), it yields

$$\begin{aligned}\mathbf{P}_\alpha\left(\overset{x}{\omega}_k,\overset{y}{\omega}_l\right)\ =&\ \overset{x}{\omega}_k{}^{M/2}\cdot\overset{y}{\omega}_l{}^{N/2}\cdot c_{k,l}\times\sum_{\substack{p=1,\ldots,M\\ q=1,\ldots,N}}\left[\mathbf{P}_\alpha\left(\overset{x}{Z}_p,\overset{y}{Z}_q\right)\overset{x}{Z}_p{}^{-M/2}\right.\\ &\left.\cdot\overset{y}{Z}_q{}^{-N/2}\cdot d_{p,q}\cdot U\left(\overset{u}{x}_k-\overset{nu}{x}_p\right)\cdot U\left(\overset{u}{y}_l-\overset{nu}{y}_q\right)\right]\end{aligned} \tag{44}$$

for $k=1,\ldots,M$ and $l=1,\ldots,N$ where

$$U(t)=\cot\left(\frac{t}{2}\right)-j \tag{45}$$

Also, $U(t)$ can be written as function of $G(t)$; indeed,

$$\begin{aligned} U(t) &= \cot\left(\frac{t}{2}\right) - j = j\frac{\left(e^{j\frac{t}{2}} + e^{-j\frac{t}{2}}\right)}{\left(e^{j\frac{t}{2}} - e^{-j\frac{t}{2}}\right)} - j \\ &= \frac{j\left(e^{jt}+1\right)}{\left(e^{jt}-1\right)} - j = \frac{2j}{e^{jt}-1} \end{aligned} \tag{46}$$

Referring to (14), we have

$$U(t) = 2jG(t) \tag{47}$$

Further, from (20), the values of the polynomial $\mathbf{P}_\alpha$ at the points $\left\{\overset{x}{Z}_p, \overset{y}{Z}_q\right\}$ for $p = 1, \ldots, M$ and $q = 1, \ldots, N$ are given as follows:

$$\begin{aligned} \mathbf{P}_\alpha\left(\overset{x}{Z}_p, \overset{y}{Z}_q\right) &= \sum_{\substack{0\le m\le M-1 \\ 0\le n\le N-1}} \alpha_{m-\frac{M}{2}, n-\frac{N}{2}} \cdot \overset{x}{Z}_p^{\,m} \cdot \overset{y}{Z}_q^{\,n} \\ &= \overset{x}{Z}_p^{\,M/2} \cdot \overset{y}{Z}_q^{\,N/2} \cdot \sum_{\substack{-\frac{M}{2}\le m \prec \frac{M}{2} \\ -\frac{N}{2}\le n \prec \frac{N}{2}}} \alpha_{m,n} \cdot \overset{x}{Z}_p^{\,m} \cdot \overset{y}{Z}_q^{\,n} \end{aligned} \tag{48}$$

Employing (19) in (48), we obtain

$$\mathbf{P}_\alpha\left(\overset{x}{Z}_p, \overset{y}{Z}_q\right) = \overset{x}{Z}_p^{\,M/2} \cdot \overset{y}{Z}_q^{\,N/2} \cdot g_{p,q} \tag{49}$$

In the same way and referring to (19) and (20), the values of $\mathbf{P}_\alpha$ at the points $\left\{\overset{x}{\omega}_k, \overset{y}{\omega}_l\right\}$ for $k = 1, \ldots, M$ and $l = 1, \ldots, N$ are given by:

$$\mathbf{P}_\alpha\left(\overset{x}{\omega}_k, \overset{y}{\omega}_l\right) = \overset{x}{\omega}_k^{\,M/2} \cdot \overset{y}{\omega}_l^{\,N/2} \cdot f_{k,l} \tag{50}$$

Using the equations (47), (49) and (50) in (44), we obtain

$$f_{k,l} = -4c_{k,l} \times \sum_{\substack{p=1,\ldots,M \\ q=1,\ldots,N}} \left[d_{p,q} \cdot G\left(\overset{u}{x}_k - \overset{nu}{x}_p\right) \cdot G\left(\overset{u}{y}_l - \overset{nu}{y}_q\right)\right] g_{p,q} \tag{51}$$

for $k = 1, \ldots, M$ and $l = 1, \ldots, N$.

And without translation, this becomes

$$f_{k,l} = \tilde{c}_{k,l} \times \sum_{\substack{p=1,\ldots,M \\ q=1,\ldots,N}} \left[\tilde{d}_{p,q} \cdot G\left(\overset{u}{x}_k - \overset{nu}{x}_p \right) \cdot G\left(\overset{u}{y}_l - \overset{nu}{y}_q \right) \right] g_{p,q} \tag{52}$$

where

$$\tilde{c}_{k,l} = -4 \cdot c_{k,l} \cdot e^{j\frac{M \times \overset{u}{x}_k}{2}} \cdot e^{j\frac{N \times \overset{u}{y}_l}{2}} \tag{53}$$

$$\tilde{d}_{p,q} = d_{p,q} \cdot e^{-j\frac{M \times \overset{nu}{x}_p}{2}} \cdot e^{-j\frac{N \times \overset{nu}{y}_q}{2}} \tag{54}$$

Until now, the calculations of $\{f_{k,l}\}_{\substack{0 \le k \le M-1 \\ 0 \le l \le N-1}}$ as function of $\{g_{p,q}\}_{\substack{0 \le p \le M-1 \\ 0 \le q \le N-1}}$ have been done only for the case of $\overset{u}{x}_k \neq \overset{nu}{x}_p$ and $\overset{u}{y}_l \neq \overset{nu}{y}_q$; therefore, we will give below its general expression taking into consideration all different cases.

Besides, adopting the form presented in (7) as well as the notations utilized in (1) up to (3) and using the Equations (19) up to (21), we obtain with the required translations:

$$f_{k,l} = \sum_{\substack{p=0,\ldots,M-1 \\ q=0,\ldots,N-1}} L_{p,q}^{k,l} \cdot g_{p,q} \tag{55}$$

for $k = 0, \ldots, M-1$ and $l = 0, \ldots, N-1$ where

$$L_{p,q}^{k,l} = \begin{cases} \zeta_{k,l} \cdot \varsigma_{p,q} \cdot G\left(\overset{u}{x}_k - \overset{nu}{x}_p \right) \cdot G\left(\overset{u}{y}_l - \overset{nu}{y}_q \right);\ \overset{nu}{x}_p \neq \overset{u}{x}_k \ \textit{and}\ \overset{nu}{y}_q \neq \overset{u}{y}_l \\ \not\zeta_k \cdot \tilde{\zeta}_l \cdot \bcancel{\varsigma}_p \cdot \tilde{\varsigma}_q \cdot G\left(\overset{u}{x}_k - \overset{nu}{x}_p \right);\ \overset{nu}{x}_p \neq \overset{u}{x}_k \ \textit{and}\ \overset{nu}{y}_q = \overset{u}{y}_l \\ \tilde{\not\zeta}_k \cdot \zeta_l \cdot \varsigma_q \cdot \tilde{\bcancel{\varsigma}}_p \cdot G\left(\overset{u}{x}_k - \overset{nu}{x}_p \right);\ \overset{nu}{x}_p = \overset{u}{x}_k \ \textit{and}\ \overset{nu}{y}_q \neq \overset{u}{y}_l \\ \tilde{\not\zeta}_k \cdot \tilde{\zeta}_l \cdot \tilde{\bcancel{\varsigma}}_p \cdot \tilde{\varsigma}_q;\ \overset{nu}{x}_p = \overset{u}{x}_k \ \textit{and}\ \overset{nu}{y}_q = \overset{u}{y}_l \end{cases} \tag{56}$$

With

$$G(t) = \frac{1}{e^{it} - 1};\ t \neq 0 \tag{57}$$

$$\zeta_{k,l} = \not\zeta_k \times \zeta_l \underbrace{\left(2i\,(-1)^k \prod_{j=1}^{M} \sin\left(\frac{\overset{u}{x}_k - \overset{nu}{x}_j}{2} \right) \right)}_{\zeta_k}$$

$$\times \underbrace{\left(2i\left(-1\right)^{l}\prod_{j=1}^{N}\sin\left(\frac{\overset{u}{y}_{l}-\overset{nu}{y}_{j}}{2}\right)\right)}_{\zeta_{l}} \tag{58}$$

$$\varsigma_{p,q} = \between_{p}\times\varsigma_{q} = \underbrace{\left(e^{\frac{-iM\overset{nu}{x}_{p}}{2}}.\tilde{\between}_{p}\right)}_{\between_{p}}\times\underbrace{\left(e^{\frac{-iN\overset{nu}{y}_{q}}{2}}.\tilde{\varsigma}_{q}\right)}_{\varsigma_{q}} \tag{59}$$

$$\tilde{\xi}_{k} = \prod_{\substack{j=1\\ j\neq p}}^{M}\sin\left(\frac{\overset{u}{x}_{k}-\overset{nu}{x}_{j}}{2}\right), \tilde{\between}_{p} = \prod_{\substack{j=1\\ j\neq p}}^{M}\frac{1}{\sin\left(\frac{\overset{nu}{x}_{p}-\overset{nu}{x}_{j}}{2}\right)}, \tag{60}$$

$$\tilde{\zeta}_{l} = \prod_{\substack{j=1\\ j\neq q}}^{N}\sin\left(\frac{\overset{u}{y}_{l}-\overset{nu}{y}_{j}}{2}\right), \tilde{\varsigma}_{q} = \prod_{\substack{j=1\\ j\neq q}}^{N}\frac{1}{\sin\left(\frac{\overset{nu}{y}_{q}-\overset{nu}{y}_{j}}{2}\right)} \tag{61}$$

In this stage, the scheme shown in Figure 2 has been well-fulfilled.

The standard algorithms* ensuring the computation of Equations (7) and (55) require each one to be over than $\mathrm{O}\left(N_T^2\right)$ $(N_T = M \times N)$ in terms of computational complexity. For that reason, we should find a fast method which permits the reduction of the computational complexity of these algorithms in order to accelerate the transition between spatial and spectral domains.

The best solution of this dilemma can be obtained by the well-known *Fast Multipole Method* (FMM)♯ [4, 31–34] which helps to compute the equations mentioned earlier in $\mathrm{O}\left(N_T \log N_T\right)$ time. Combining the FMM with 2D-LIF, the transition between the coefficients defined with equispaced data $\{f_{k,l}\}$ and the one with unequally data $\{g_{p,q}\}$ will be called, henceforth, *two-dimensional fast interpolation transform* (2D-FIT).

With the efficiency of the FFT algorithm in terms of the computational complexity, the transformation between spatial and Fourier domains can be, therefore, obtained in $\mathrm{O}\left(N_T \log N_T\right)$ time while taking into consideration the non-uniformly input data. This transformation constitutes the 2D-NUFFT.

Figure 3 and Figure 4 summarize how the 2D-NUFFT and 2D-INUFFT were built.

---

* We will assume that these algorithms are chosen without any fast procedures.

♯ This method has been applied already to Finite Element Method for investigation of large scattering problems [35].

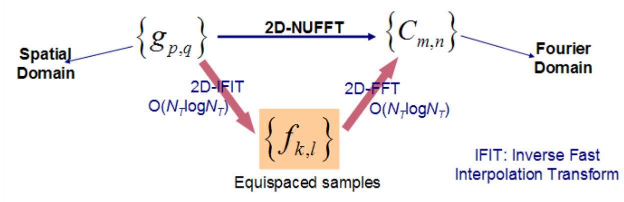

Figure 3. Scheme of 2D-non-uniform fast fourier transform.

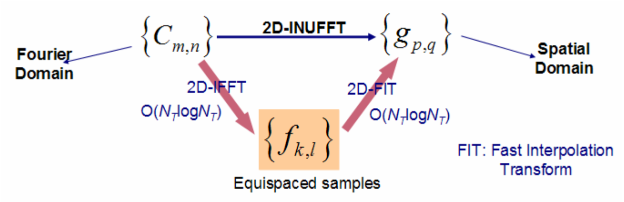

Figure 4. Scheme of 2D-inverse non-uniform fast fourier transform.

4. 2D-NUFFMT AND TWA IN NOVEL VERSION

Based on the results obtained in the previous section, we can deduce that the presence of FFT and IFFT in, respectively, 2D-NUFFT and its inverse allows us to straightforwardly apply the FMT and IFMT (already developed in [1]) respectively.

The combination between these components (2D-NUFFT+FMT and 2D-INUFFT+IFMT) forms a novel transformations so-called two-dimensional non-uniform fast Fourier mode transform (2D-NUFFMT) and its inverse 2D-INUFFMT which constitute together the central component of the novel version of TWA method. The figure depicted in Figure 5 illustrates the different transformations from spatial domain to modal domain of vector **V** defined on non-uniform discretization and gives a panorama upon TWA process in its novel version††.

5. THE ADOPTED FORMALISM ON THE MESH IN TWA$^+$ PROCESS

It is clear that the definition of meshing resolution represents one of the strongest parameters which allow us to conclude on the speediness of TWA process.

†† To differentiate from its conventional version, the novel TWA based on 2D-NUFFMT will be called the *advanced TWA* and abbreviated by *TWA*$^+$.

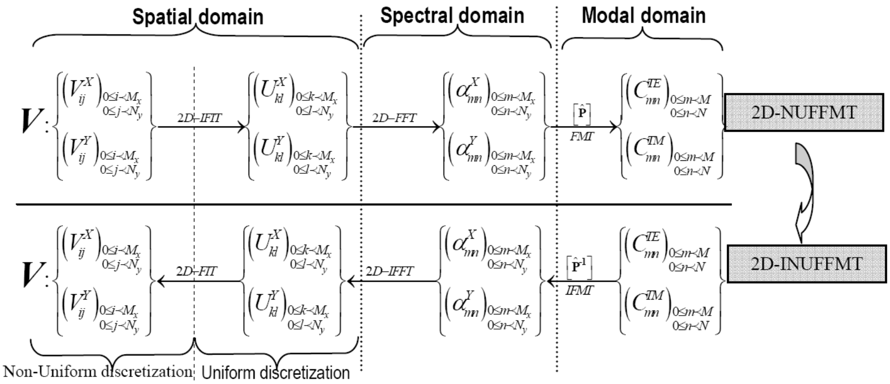

Figure 5. General prospect on 2D-NUFFMT and its inverse.

Therefore, it is important to carefully define, in TWA$^+$ process, the total number of cells characterizing the air-dielectric interface. This can be achieved, whatsoever the type of mesh is used (i.e., equally or unequally input data), by adopting a meshing effective technique (MET) in TWA$^+$ code. In what follows, we will illustrate, throughout example of simple planar structure, the different steps constituting the appropriate procedure based on MET during its implementation in TWA$^+$ code.

5.1. Setp1

Initially, we should start with a suitable total number of pixels $M \times N$ defining the discontinuity surface such as these cells are uniform as used in conventional TWA process. It should be noted that the meshing resolution must be in good quality in order to obtain a rigorous analysis of any considered circuit. Figure 6 exhibits an example of patch antenna studied with two different uniform mesh: 16×16 (Figure 6(a)) and 64×64 (Figure 6(b)). The latter resolution is preferred and taken in this first step for TWA$^+$ process as well as in full-analysis using conventional TWA.

5.2. Setp2

Next and during the execution of TWA$^+$ code, the total number of pixels $M \times N$ is modified and the discretization becomes non-uniform (This option is absent in conventional TWA process.) by applying the refinement mesh *only* on the surface defining the analysis circuit. This allows an important reduction on total number of cells while keeping

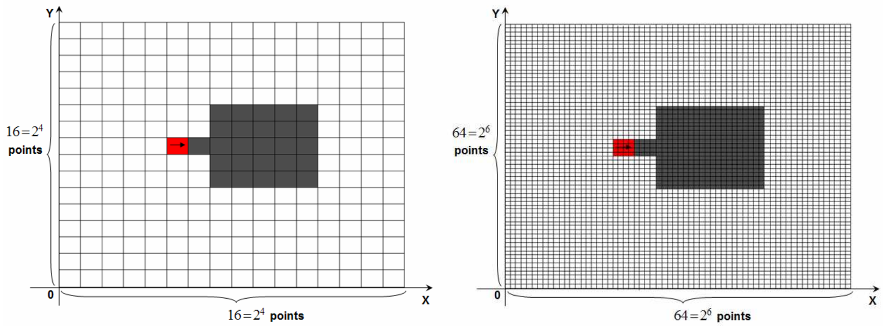

Figure 6. Planar structure studied with two different uniform meshes: 16×16 ((a)) and 64×64 ((b)).

a good resolution for simulation. The example below clarifies this step. Indeed, applying the mesh only on the patch antenna shown in Figure 6(a) by adopting the resolution presented in Figure 6(b), we obtain a good resolution with a minimum total number of pixels as depicted in Figure 7.

However, three mesh categories have been applied: the first represents a refinement uniform mesh on the surface characterizing the considered circuit (i.e., application of small uniform pixels on the circuit's domain) given by zone 1, the second defines other uniform mesh-size as shown in zone 2, and the last delineates a regular mesh everywhere else (i.e., outside the circuit's domain) as depicted in zone 3. Form this, a discontinuity of cells (i.e., sudden change between two different cells mainly on the region close to circuit's domain) is observed as shown in Figure 7. Such can affect the good analysis of considered circuit.

5.3. Setp3

In order to tackle the problem mentioned earlier, we propose an adaptive refinement mesh allowing a suitable graduation on the mesh in the change from small pixel to another greater essentially in the regions close to circuit's domain so as to avoid the sudden change between pixels as shown in Figure 8. The density of non-uniform cells in this case becomes important compared to the one presented in previous step.

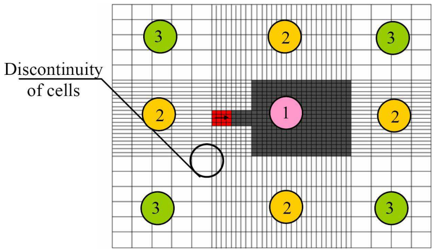

Figure 7. Refinement mesh only on the surface defining the analysis circuit and discontinuity of cells.

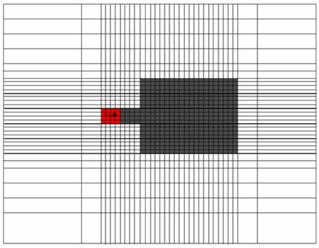

Figure 8. Adaptive refinement mesh applied to analysis structure.

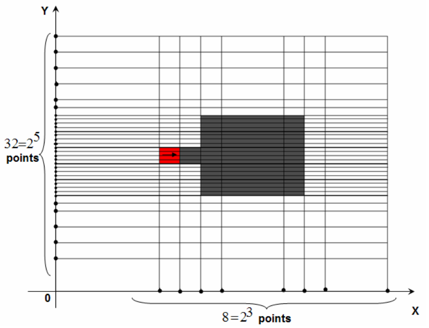

Figure 9. Adaptive refinement mesh applied to analysis structure.

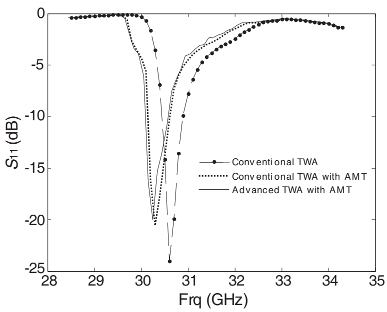

Figure 10. S_{11} of 30 GHz patch antenna by three different versions of TWA method.

5.4. Setp4

To this end, the final total number of pixels considered for TWA$^+$ process must be an integer to the power of 2. Therefore, combining the adaptive refinement mesh with AMT technique mentioned already in [1], we implement a sub-procedure making sure that the total number of cells in x as well as in y is always an integer to the power of 2 before full-wave analysis of the considered circuit. The following figure shows the final mesh considered in TWA$^+$ process for investigation of patch antenna.

It is remarkable that the total number of pixels presented in Figure 6(a) is equal to the one depicted in Figure 9. Yet, an important gap can be observed between them in the quality of simulations results.

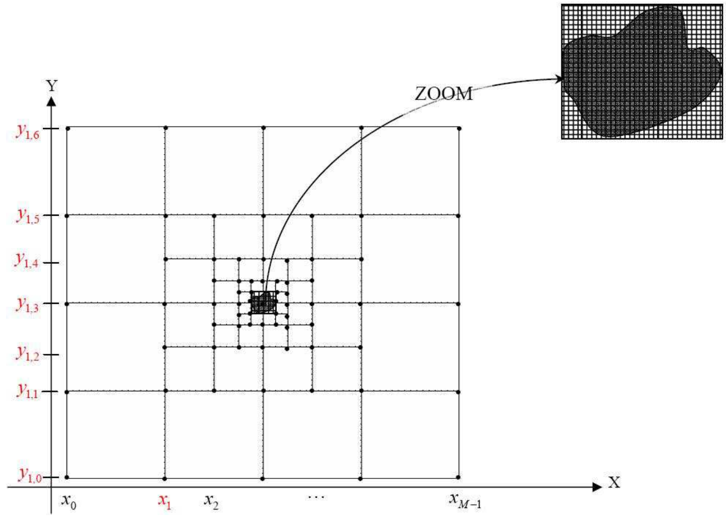

Figure 11. Well configured arbitrary meshing for 2D-NUDFT algorithm.

6. APPLICATION EXAMPLE FOR WIRELESS SYSTEMS

In order to show the efficiency of our work developed above, the 30 GHz patch antenna used in wireless applications already investigated in [1] has been considered as application example for full-wave analysis taking into consideration their geometric and modeling parameters given in Table 2 presented also in [1].

On the one hand, pick up again the results obtained in [1] related to the return loss for the 30 GHz patch antenna. This antenna was simulated by both conventional TWA with and without AMT technique adopting, respectively, as meshing resolution 256×256 and 16×256 and the obtained simulation results have shown a full agreement between them. So, a considerable gain in CPU computation time has been achieved for conventional TWA with AMT compared to the one without AMT.

On the other hand, we run the considered 30 GHz patch antenna on TWA$^+$ code. It should be noted that the final total number of non-uniform pixels chosen for implementation is 8×64. The simulation result characterizing the evolution of S11 parameter in decibel versus frequency (i.e., return loss) is favorably compared (error 0.5% approx.) to the result obtained with 'conventional TWA with AMT' as depicted in Figure 10.

Furthermore, the execution time in TWA^+ process for the simulation of this antenna is almost seven times faster than the consumed time in conventional TWA process where the AMT technique is applied in both cases.

7. CONCLUSION

In this paper, an advanced TWA (TWA^+) based on two-dimensional non-uniform fast Fourier mode transform has been presented, developed and successfully implemented for full-wave investigation of microwave structure. A detailed description of the procedure explaining the mesh handling adopted in TWA^+ process has been presented. The obtained simulation results for applications belonging to wireless systems have been favorably compared showing the efficiency and the speediness of TWA^+ compared to the conventional TWA even if in presence of AMT technique in the context of EM simulations.

Further, this work can be improved by the implementation of a fast parallel algorithm computing the non-equispaced fast Fourier transform on commodity graphics hardware (the GPU). This can be achieved by referring to [36].

Although their efficacy and rapidity, TWA^+ method presents some shortcomings mainly at the manipulation of mesh on the surface discontinuity. Indeed, the arbitrary mesh which is a significant parameter in CPU computation time cannot be treated with this method. For that reason, the two-dimensional non-uniform discrete Fourier transform (2D-NUDFT) in matrix form can be implemented in TWA process offering the possibility to handle this meshing with suitable configuration according to the studied circuit as depicted in Figure 11. Referring to [25], the 2D-NUDFT for the well configured arbitrarily meshing can be accomplished by an extension of the studied case 'Non-uniform Sampling on Parallel Lines' presented in the latter reference following the structure shown in Figure 11. Vandermonde matrices [37] must be manipulated in this case in order to find the inverse of 2D-NUDFT easily. To this end, the existence of very large matrices which may make TWA very slower allows us to call some fast algorithms such as Fast Multi-resolution Algorithms for Matrix-Vector Multiplication [38], Fast Matrix Multiplication Algorithms [39] and Fast Multiplication of larges matrices using wavelets [40, 41] in view of the much presence of the sparse matrices (large matrices with a high percentage of zero-valued elements) in the RFIC applications.

ACKNOWLEDGMENT

The authors would like to thank professors Slimane Adjerid and David Russell in the department of mathematics at Virginia tech for their comments and suggestions to improve the quality of this work.

REFERENCES

1. Ayari, M., T. Aguili, and H. Baudrand, "More efficiency of Transverse Wave Approach (TWA) by applying Anisotropic Mesh Technique (AMT) for full-wave analysis of microwave planar structures," *Progress In Electromagnetics Research B*, Vol. 14, 383–405, 2009.
2. Ayari, M., T. Aguili, H. Temimi, and H. Baudrand, "An extended version of Transverse Wave Approach (TWA) for full-wave investigation of planar structures," *Journal of Microwave, Optoelectronics and Electromagnetic Applications*, Vol. 7, No. 2, Dec. 2008.
3. Brigham, E. O., *The Fast Fourier Transform*, Prentice-Hall, NJ, 1974.
4. Dongarra, J. and F. Sullivan, "Introduction to the top 10 algorithms," *Computing in Science and Engineering*, Vol. 2, No. 1, 2000.
5. Cooley, J. W. and J. W. Tukey, "An algorithm for machine calculation of complex fourier series," *Math. Computation*, Vol. 19, No. 90, 297, 1965.
6. Sundararajan, D., *The Discrete Fourier Transform: Theory, Algorithms and Applications*, Prentice-Hall, NJ, 2001.
7. Anderson, C. and M. D. Dahleh, "Rapid computation of the discrete Fourier transform," *SIAM J. Sci. Comput.*, Vol. 17, 913–919, 1996.
8. Oppenheim, A. and D. Johnson, "Computation of spectra with unequal resolution using the fast Fourier transform," *Proc. IEEE*, Vol. 59, 299–301, Feb. 1971.
9. Bagchi, S. and S. Mitra, *The Nonuniform Discrete Fourier Transform and Its Applications in Signal Processing*, Kluwer, Boston, MA, 1999.
10. Bagchi, S. and S. K. Mitra, "The nonuniform discrete Fourier transform and its applications in filter design. 1 — 1-D," *IEEE Trans. Circuits Syst. 2*, Vol. 43, 422–433, Jun. 1996.
11. Angelides, E. and J. E. Diamessis, "A novel method for designing FIR digital filters with non-uniform frequency samples," *IEEE*

Trans. Acoust., Speech, Signal Processing, Vol. 42, 259–267, Feb. 1994.

12. Angelides, E., "A recursive frequency-sampling method for designing zero-phase FIR filters by nonuniform samples," *IEEE Trans. Signal Processing*, Vol. 6, 1461–1467, Jun. 1995.
13. Sutton, B. P., D. C. Noll, and J. A. Fessler, "Fast, iterative image reconstruction for MRI in the presence of field inhomogeneities," *IEEE Trans. Med. Imag.*, Vol. 22, No. 2, 178–188, Feb. 2003.
14. Sutton, B. P., J. A. Fessler, and D. Noll, "A min-max approach to the non-uniform N-D FFT for rapid iterative reconstruction of MR images," *Proc. Int. Soc. Mag. Res. Med.*, 763, 2001.
15. Brouw, W. N., "Aperture synthesis," *Methods in Computational Physics*, B. Alder, S. Fernbach, and M. Rotenberg (eds.), Vol. 14, 131–175, 1975.
16. O'Sullivan, J. D., "A fast sinc function gridding algorithm for Fourier inversion in computer tomography," *IEEE Trans. Med. Imag.*, Vol. 4, No. 4, 200–207, 1985.
17. Fourmont, K., "Non-equispaced fast Fourier transforms with applications to tomography," *J. Fourier Anal. Appl.*, Vol. 9, No. 5, 431–450, 2003.
18. Lawton, W., "A new polar Fourier-transform for computer-aided tomography and spotlight synthetic aperture radar," *IEEE Transactions on Acoustics Speech and Signal Processing*, Vol. 36, No. 6, 931–933, Jun. 1988.
19. Kaveh, M. and M. Soumekh, "Computer-assisted diffraction tomography," *Image Recovery: Theory and Application*, H. Stark (ed.), 369–413, 1987.
20. Dutt, A. and V. Rokhlin, "Fast Fourier transforms for nonequispaced data," *SIAM J. Sci. Comput.*, Vol. 14, 1368–1393, Nov. 1993.
21. Dutt, A. and V. Rokhlin, "Fast Fourier transforms for nonequispaced data 2," *Appl. Comput. Harmon. Anal.*, Vol. 2, 85–100, 1995.
22. Beylkin, G., "On the fast fourier-transform of functions with singularities," *Appl. Comput. Harmon. Anal.*, Vol. 2, No. 4, 363–381, Oct. 1995.
23. Steidl, G., "A note on fast Fourier transforms for nonequispaced grids," *Advances in Computational Mathematics*, Vol. 9, 337–352, 1998.
24. Potts, D., G. Steidl, and M. Tasche, "Fast Fourier transforms for nonequispaced data: A tutorial," *Modern Sampling Theory:*

Mathematics and Applications, J. J. Benedetto and P. Ferreira (eds.), 249–274, Birkhäuser, Boston, MA, 2001.

25. Bagchi, S. and S. K. Mitra, "The nonuniform discrete Fourier transform and its applications in filter design. 2 — 2-D," *IEEE Trans. Circuits Syst. 2*, Vol. 43, 434–444, Jun. 1996.
26. Su, K. Y. and J. T. Kuo, "A two-dimensional nonuniform fast Fourier transform (2-D NUFFT) method and its applications to the characterization of microwave circuits," *Asia-Pacific Microwave Conf.*, 801–804, Seoul, Korea, Nov. 4–7, 2003.
27. Su, K. Y. and J. T. Kuo, "Application of Two-Dimensional Non-uniform Fast Fourier Transform (2-D NUFFT) technique to analysis of shielded microstrip circuits," *IEEE Transactions on Microwave Theory and Techniques*, Vol. 53, No. 3, Mar. 2005.
28. Liu, Q. H., X. M. Xu, B. Tian, and Z. Q. Zhang, "Applications of nonuniform fast transform algorithms in numerical solutions of differential and integral equations," *IEEE Trans. Geosci. Remote Sensing*, Vol. 38, No. 4, 1551–1560, Jun. 2000.
29. Stoer, J. and R. Bullirsch, *Introduction to Numerical Analysis*, Springer-Verlag, New York, 1980.
30. Yazici, A., I. Altas, and T. Ergenc, "2D polynomial interpolation: A symbolic approach with mathematica," *Lecture Notes in Computer Science (LNCS)*, O. Gervasi et al. (eds.), ICCSA, Vol. 3482, 463–471, Springer-Verlag Berlin Heidelberg, 2005.
31. Board, J. and K. Schulten, "The fast multipole algorithm," *Computing in Science and Engineering 2*, Vol. 1, 76–79, 2000.
32. Raykar, V. C., "A short primer on the fast multipole method: FMM tutorial," University of Maryland, College Park, Apr. 8, 2006.
33. Coifman, R., V. Rokhlin, and S. Wandzura, "The fast multipole method for the wave equation: A pedestrian prescription," *IEEE Antennas Propagat. Mag.*, Vol. 35, 7–12, Jan. 1993.
34. Song, J. M. and W. C. Chew, "Multilevel fast-multipole algorithm for solving combined field integral equations of electromagnetic scattering," *Microw. Opt. Technol. Lett.*, Vol. 10, 15–19, 1995.
35. Wei, X.-C., E. P. Li, and Y. J. Zhang, "Application of the improved finite element-fast multipole method on large scattering problems," *Progress In Electromagnetics Research*, PIER 47, 49–60, 2004.
36. Sørensen, T. S., T. Schaeffter, K. Ø. Noe, and M. S. Hansen, "Accelerating the non-equispaced fast fourier transform on commodity graphics hardware," *IEEE Transactions on Medical*

and Imaging, Vol. 27, No. 4, Apr. 2008.

37. Turner, L. R., "Inverse of the vandermonde matrix with applications," *NASA*, Washington, D.C., Aug. 1966.
38. Electe, A. H. and I. Yad-Shalom, "Fast multi-resolution algorithms for matrix vector multiplication," Institute for Computer Applications in Science and Engineering, NASA Langley Research Center, Hampton, Virginia, Oct. 1992.
39. Nguyen, D. K., I. Lavall'ee, and M. Bui, "A general scalable implementation of fast matrix multiplication algorithms on distributed memory computers," *Proceedings of the Sixth International Conference on Software Engineering, Artificial Intelligence, Networking and Parallel/Distributed Computing and First ACIS International Workshop on Self-Assembling Wireless Networks (SNPD/SAWN'05)*, 2005.
40. Bond, D. M. and S. A. Vavasis, "Fast wavelet transforms for matrices arising from boundary elements methods: Tutorial," Center for Applied Mathematics, Engineering and Theory Center, Cornell University, Ithaca, NY, Mar. 25, 1994.
41. "Fast multiplication of large matrices," Wavelet Applications (Wavelet Toolbox), Matlab7.1.
42. Liu, Q. H. and X. Y. Tang, "Iterative algorithm for nonuniform inverse fast Fourier transform (NU-IFFT)," *Electronics Letters*, Vol. 34, No. 20, 1913–1914, 1998.